Using Power Line Communication for Fault Detection and Localization in Star-shaped Network

Abdelkarim Abdelkarim, Virginie Degardin, Mohamed Amine Atoui, Vincent Cocquempot

Available online at www.sciencedirect.com

ScienceDirect

IFAC PapersOnLine 55-6 (2022) 526–532

Using Power Line Communication for Fault Detection and Localization in Star-shaped Network

Abdel Karim Abdel Karim[1,2] **Atoui M. Amine**[1,2]
Degardin Virginie[1] **Cocquempot Vincent**[2]

[1] *Univ. Lille, CNRS, Centrale Lille, Univ. Polytechnique Hauts-de-France, UMR 8520 - IEMN, F-59000 Lille, France*
[2] *Univ. Lille, CNRS, Centrale Lille, UMR 9189 - CRIStAL, F-59000 Lille, France*
e-mail: abdel-karim.abdel-karim@univ-lille.fr, amine.atoui@gmail.com and virginie.degardin@univ-lille.fr, vincent.cocquempot@univ-lille.fr

Abstract: In energy or communication networks, cables are omnipresent. Like any other systems, they are subject to faults. Faults in cables are divided into two families : *soft* faults and *hard* faults. Soft faults are faults that do not affect the data and/or energy transfer. However, over time they tend to turn into hard faults that can lead to a total system breakdown. In this paper, we focus on the detection of soft faults and the localization of the faulty branch in star-shaped networks. The proposed method is based on the comparison between a network Reference Transmission Coefficient (RTC) and a TC measured online through power line communication using Orthogonal Frequency Division Multiplexing (OFDM) scheme. Our proposal is discussed for both energy and communication networks. Simulation-based results are presented that confirm the ability of the method to locate the faulty branches.

Keywords: Health monitoring, Power line communication, Fault detection, Fault localization, Star-shaped Network.

1. INTRODUCTION

Monitoring the health of technological systems is of paramount importance to maintain high quality of service and product. Unfortunately, communication and energy cables are often ignored in such monitoring tasks. According to statistics from some automotive original equipment manufacturers, 70% of returned Electronic Control Units (ECUs) were tested flawless, which implies that the faults were in the cables (Auzanneau, 2013). These faults can be divided into two types : *soft faults* and *hard faults*, depending on their degree of severity. A fault usually appears as a superficial fault called soft fault which evolves with time to a more severe fault called hard fault. Therefore, fault detection and localization techniques focus on detecting and localizing soft faults before they become hard faults that can impact the system behavior. Most fault detection and localization methods, known as reflectometry methods, rely on high frequency reflection analysis. A review of these reflectometry methods is presented in (Furse et al., 2020). To measure and analyze the reflection due to impedance discontinuities, special heavy and expensive equipment must be installed on the network (Dubickas, 2006). To avoid the use of additional instruments, alternative methods based on the use of already installed Power Line Communication (PLC) modems are proposed in (Yang et al., 2013), (Lehmann et al., 2016), (Lallbeeharry et al., 2018) and (Huo et al., 2019) to detect soft faults. The methods that rely on the use of PLC have almost the same concept, namely the comparison between the Reference Transmission Coefficient (RTC), estimated in a healthy network, and the Transmission Coefficient (TC) estimated online through PLC using Orthogonal Frequency Division Multiplexing (OFDM). A fault is detected when the TC deviates from the RTC. The methods of comparison between the RTC and the successive TC can be based on either monitoring the values and positions of peaks and notches (Yang et al., 2013), using different machine learning techniques (Huo et al., 2019), using neural networks (Huo et al., 2020) or on using correlation coefficients (Lallbeeharry et al., 2018). A PLC-based method for detecting and locating the faulty branch in a bus network was presented in (Abdel Karim et al., 2021c) and (Abdel Karim et al., 2021a). This method was validated using real measurement extracted from a Y-shaped network in (Abdel Karim et al., 2021b).

In that paper, the same approach is used to detect then locate single and multiple faults in star-shaped networks which are extensively used in communication and energy transfer systems. PLC is used to estimate the RTC and the successive TC that need to be tested for fault detection. Residuals deduced from the chain matrix modeling approach are proposed and used to detect and to locate faulty branches. In section 2, the two types of star-shaped net-

⋆ This research work is done in the framework of the ELSAT2020 project which is co-financed by the European Union with the European Regional Development Fund, the French state and the Hauts-de-France Region Council.

10.1016/j.ifacol.2022.07.182

works are presented. Afterwards, a deterministic modeling approach is used to model networks in section 3. Then, the fault detection and localization method using TC-based residuals is detailed in section 4. The proposed method is validated by simulations in section 5. Conclusions and future work close this paper.

2. STAR NETWORKS

Physical topology is founded on the physical connections of cables and devices. In a star-shaped network, all components are individually linked to a central component. The central component can be a hub, a switch, an Electronic Control Unit (ECU) or even a simple connector (Espina et al., 2014).
Two different types of star topology are studied in this paper : a Star-shaped Energy Network (SEN) and a Star-shaped Communication Network (SCN).

A Star-shaped Energy Network (SEN) is presented in Fig. 1-(a). All ECUs are connected to a central node. The node is considered as a simple connector. If one of the ECUs wants to communicate with another one through PLC, the message will be sent directly and will be transmitted to all the other ECUs.

A Star-shaped Communication Network (SCN) is presented in Fig. 1-(b). All the ECUs denoted as slaves are connected to a central or master ECU. A point-to-point connection is established between the source, S, and each of the receivers, R_i, separately. If one of the ECUs wants to communicate with another, it sends the message to the master ECU, which in turn repeats the message and sends it to the targeted ECU.

The two networks are composed of a source S, $N+1$ receivers where R_i denotes the i^{th} receiver.

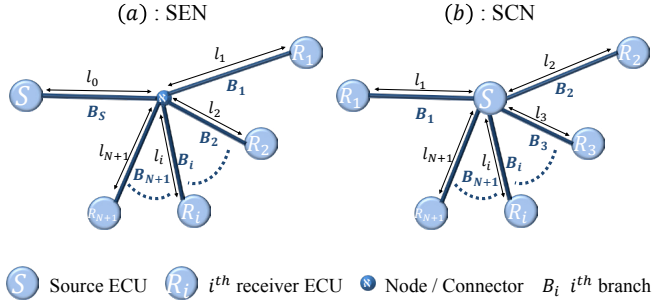

Fig. 1. Representation of a SEN and a SCN.

3. NETWORK MODELING

A deterministic modeling approach, based on the transmission chain matrices (Mlỳnek et al., 2011), is used to model the channel between the source and each receiver of the network. A transmission line with the length l, a characteristic impedance Z_c and a propagation constant γ is considered as a two-port network. The voltage and current at the output of the line : U_2 and I_2, are linked to those at the input of the line : U_1 and I_1 by the transmission chain matrix M (Paul, 2007).

$$M(l) = \begin{bmatrix} \boldsymbol{a} & \boldsymbol{b} \\ \boldsymbol{c} & \boldsymbol{d} \end{bmatrix} = \begin{bmatrix} ch(\gamma l) & Z_c \cdot sh(\gamma l) \\ \dfrac{1}{Z_c} \cdot sh(\gamma l) & ch(\gamma l) \end{bmatrix} \quad (1)$$

$$\begin{bmatrix} U_1 \\ I_1 \end{bmatrix} = M(l) \times \begin{bmatrix} U_2 \\ I_2 \end{bmatrix} \quad (2)$$

The transmission coefficient, $H(f)$, of the transmission line can be computed using (3) under the condition of matched impedance ($Z_R = Z_s = Z_c$) (Bahl, 2009).

$$H(f) = \frac{U_2 + Z_R \cdot I_2}{U_1 + Z_s \cdot I_1} = \frac{2}{\boldsymbol{a} + \frac{\boldsymbol{b}}{Z_c} + \boldsymbol{c} \cdot Z_c + \boldsymbol{d}} \quad (3)$$

where f denotes the frequency, Z_R and Z_s are respectively the impedances of the receiver and the source at the output and the input of the line, Z_c is the characteristic impedance of the line, $\boldsymbol{a}$, $\boldsymbol{b}$, $\boldsymbol{c}$ and $\boldsymbol{d}$ are the parameters of the transmission chain matrix.

3.1 Star-shaped energy network modeling

A SEN, as seen in Fig. 2, is composed of a source S, $N+1$ receivers ($R_i \; \forall \; i \; \in \{1; 2; \ldots; N+1\}$), $N+2$ branches and a node.

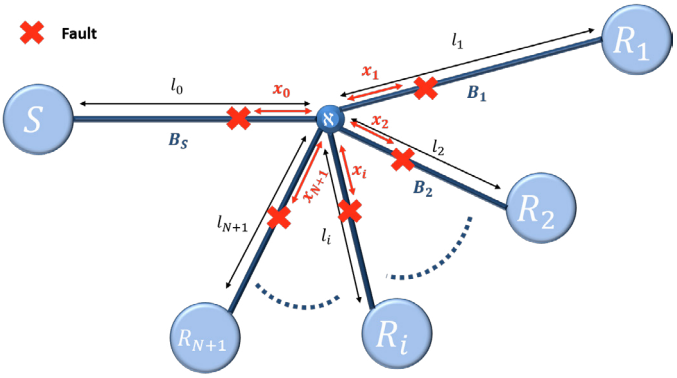

Fig. 2. Star-shaped energy network.

The chain matrix M_{R_i} between the source and the i^{th} receiver, R_i, is the product of three cascaded matrices. The first one represents the branch between the source and the node, the second one represents all the branches extended from the node (except the branch B_i) and the last one represents the branch B_i between the node and the receiver R_i. All the branches extended from the node can be represented by an equivalent parallel impedance Z_p.

$$M_{R_i} = M(l_0) \times P(Z_p) \times M(l_i) \quad (4)$$

where $P(Z_p)$ represents the matrix of a parallel impedance Z_p, $M(l_0)$ represents the matrix of the branch B_S and $M(l_i)$ represents the matrix of the branch B_i.

$$P(Z_p) = \begin{bmatrix} 0 & 0 \\ \dfrac{1}{Z_p} & 0 \end{bmatrix} \quad (5)$$

where Z_p is the equivalent parallel impedance representing all the branches extended from the node except B_i. It can be computed using (6).

$$\frac{1}{Z_p} = \sum_{j=1}^{N} \frac{1}{Z_{eq_j}}; \quad j \neq i \quad (6)$$

where Z_{eq_j} is the equivalent impedance of the branch B_j and of the receiver R_j at its end. It is computed using (7).

$$Z_{eq_j} = \frac{\boldsymbol{a_j} \cdot Z_{R_j} + \boldsymbol{b_j}}{\boldsymbol{c_j} \cdot Z_{R_j} + \boldsymbol{d_j}} \tag{7}$$

where $\boldsymbol{a_j}$, $\boldsymbol{b_j}$, $\boldsymbol{c_j}$ and $\boldsymbol{d_j}$ are the parameters of the matrix representing the branch B_j and Z_{R_j} is the impedance at its extremity.
Under the condition of matched impedance ($Z_{R_i} = Z_c \; \forall \; i \in \{1; 2; \ldots; N+1\}$), $Z_{eq_j} = Z_c$ and the equivalent parallel impedance $Z_p = \frac{Z_c}{N}$. The transmission coefficient, $H_{R_i}(f)$, between the source S and the receiver, R_i, is computed using (3):

$$H_{R_i}(f) = \frac{2}{(2+N) \cdot e^{\gamma(l_0+l_i)}} \tag{8}$$

According to (Sommervogel, 2020), moisture inside a connector or series arc have the same effect as adding a lumped series impedance Z_f that leads to a smooth variation of the cable characteristic impedance. In Fig. 2, several possible fault positions are presented : faulty branch B_S, faulty branch B_1, ..., B_{N+1}. The faulty branch, B_i of length l_i may be divided into three parts, one part prior to the fault's position represented by $M(x_i)$, another part representing the fault itself, $F(Z_f)$, and a part posterior to the fault's position represented by $M(l_i - x_i)$ where x_i the distance between the fault's position and the node. As a consequence, the transmission chain matrix M_f of a faulty branch, B_i, of length l_i can be expressed as:

$$M_f(l_i, x_i) = M(x_i) \times F(Z_f) \times M(l_i - x_i) \tag{9}$$

$F(Z_f)$ denotes the chain matrix representing the lumped series impedance Z_f representing the fault's severity which can be expressed as:

$$F(Z_f) = \begin{bmatrix} 0 & Z_f \\ 0 & 0 \end{bmatrix} \tag{10}$$

Using the above information, the transmission coefficient between the source and each receiver in all possible single faulty branch cases of the network are computed and presented in table 1.

3.2 Star-shaped communication network modeling

A SCN, as shown in Fig. 3, is composed of a source S and $N+1$ receivers ($R_i \; \forall \; i \in \{1; 2; \cdots; N+1\}$). A point-to-point connection is established between the source and each receiver R_i.

Healthy case : the chain matrix representing a healthy branch between the two ECUs (S and R_i) is denoted as $M^h_{R_i}$.

$$M^h_{R_i} = M(l_i) \tag{11}$$

The transmission coefficient, $H^h_{R_i}$, between S and R_i is computed using (3).

$$H^h_{R_i}(f) = \frac{1}{e^{\gamma l_i}} \tag{12}$$

Faulty case : the chain matrix representing a faulty branch between S and R_i is denoted as $M^f_{R_i}$.

$$M^f_{R_i} = M_f(l_i, x_i) \tag{13}$$

The transmission coefficient, $H^f_{R_i}$, between S and R_i is computed using (3).

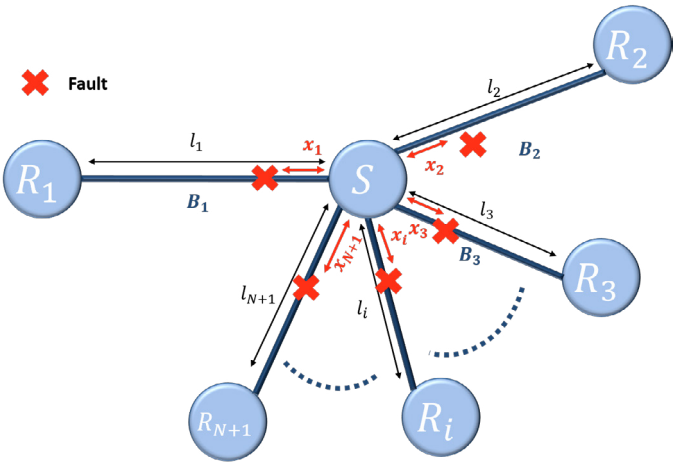

Fig. 3. Star-shaped communication network.

$$H^f_{R_i}(f) = \frac{2}{(2 + \frac{Z_f}{Z_c}) \cdot e^{\gamma l_i}} \tag{14}$$

The influence of the fault is limited to the receiver directly linked to the faulty branch. The fault has no impact on the other receivers. Thus, the expression of the transmission coefficient between the source and a receiver is either equal to $H^h_{R_i}(f)$ or equal to $H^f_{R_i}(f)$ depending on the state of health of the cable linking these two ECUs.

4. FAULT DETECTION AND LOCALIZATION METHOD

The proposed Fault Detection and Localization (FDL) method is based on a set of residuals. One residual can be computed at each receiver R_i after estimating the transmission coefficient, H_{R_i}, between the source and R_i. The proposed residual, $\rho_{R_i}(f)$, computed at the receiver R_i is expressed as:

$$\rho_{R_i}(f) = \left| \frac{H^{Ref}_{R_i}(f)}{H^{Test}_{R_i}(f)} \right| - 1 \tag{15}$$

$H^{Ref}_{R_i}(f)$ denotes the RTC between the source and R_i, estimated when the network is considered as healthy. $H^{Test}_{R_i}(f)$ is the TC between the source and the receiver R_i that needs to be tested for fault.
If the network is healthy, the estimated TC is equal to the RTC. Thus, $\rho_{R_i}(f)$ is null. If the network is faulty, the estimated TC is different from the RTC. Thus, $\rho_{R_i}(f)$ is different from zero.
To estimate $H^{Ref}_{R_i}(f)$ and $H^{Test}_{R_i}(f)$, a reference symbol in the frequency domain, $X_{f_k,n}$, known by the transmitter (source) and the receiver is used (Hsieh and Wei, 1998), where $X_{f_k,n}$ is the n^{th} symbol at the k^{th} frequency component. The principle of TC estimation is as follows: the source sends to the receiver known symbols called *pilot symbols* in the frequency domain. Upon receiving these known symbols, the receiver estimates the TC between the transmitted symbol, $X_{f_k,n}$, and the received one, $Y_{f_k,n}$, using (16):

$$\hat{H}(f_k) = \frac{1}{N_t} \sum_{n=1}^{N_t} \frac{Y_{f_k,n}}{X_{f_k,n}} \quad k \in [0, W-1] \tag{16}$$

Table 1. Transmission coefficients between the source and each receiver, R_i, in all the possible single faulty cases of the SEN.

	Healthy (Reference)	Faulty B_S	Faulty B_i (Branch connected to R_i)	Faulty B_j $(j \neq i)$
$H_{R_i}(f)$	$\frac{2}{(2+N)\cdot e^{\gamma(l_0+l_i)}}$	$\frac{2}{(2+N)\cdot e^{\gamma(l_0+l_i)}+A(x_0,l_i)}$	$\frac{2}{(2+N)\cdot e^{\gamma(l_0+l_i)}+A(x_i,l_i)}$	$\frac{2}{(2+N)\cdot e^{\gamma(l_0+l_i)}+B(x_j,l_i)}$

With $A(x,l) = e^{\gamma(l_0+l)} \cdot \frac{Z_f}{2\cdot Z_c} \cdot (2 + N(1 + e^{-2\cdot\gamma\cdot x}))$, $B(x,l) = e^{\gamma(l_0+l)} \cdot (\lambda_f(x) - N)$

where $\lambda_f(x) = \frac{2N\cdot Z_c + Z_f\cdot(N+(N-2)\cdot e^{-2\cdot\gamma\cdot x})}{2\cdot Z_c + Z_f\cdot(1+e^{-2\cdot\gamma\cdot x})}$ and $i,\, j \in \{1;2;\ldots;N+1\}$

where f_k is the k^{th} frequency component, W is the number of the frequency components, $\hat{H}(f_k)$ is the estimated TC, N_t is the number of symbols and n is the symbol number.

Single and multiple faults are explored for both networks (SEN and SCN) to show the pertinence of the proposed residual.

4.1 FDL on a star-shaped communication network (SCN)

In a SCN, a point-to-point connection is established between each ECU and the central/master ECU. Therefore, two main situations of the network are distinguished, the healthy and the faulty situations.

Healthy situation : When the network is considered as healthy, the successive measurements of the transmission coefficient are equal to the reference transmission coefficient. Thus, the residual computed using (15) is

$$\rho_{R_i}(f) = 0 \;\forall\; i \;\in\; \{1;2;\ldots;N+1\} \tag{17}$$

Faulty situation : When a fault occurs, only the receiver directly linked to the faulty branch is influenced. Single and multiple fault scenarios are distinguished.

(1) Single faults scenarios in the faulty branch B_j : The transmission coefficient between the source and R_j will deviate from the RTC. However, the transmission coefficient estimated between the source and each receiver R_i with $i \neq j$ is equal to its RTC. Thus, the residuals computed using (15) are

$$\rho_{R_j}(f) \neq 0 \tag{18}$$

$$\rho_{R_i}(f) = 0 \;\forall\; i \;\in\; \{1;2;\ldots;N+1\} - \{j\} \tag{19}$$

The localization of the fault is straightforward. Once the fault is detected by one of the receiver, the faulty branch B_j is located. Only the TC between the source and the receiver R_j is affected. The other estimated TCs between the source and the receiver $R_j (j \neq i)$ are respectively identical to their RTCs.

(2) Multiple faults scenarios : Since a fault in one of the branches of a SCN has only an influence on the receiver directly linked to that particular branch, multiple faults are detected and located the same way as single fault. Thus, the residuals computed using (15) are

$$\rho_{R_i}(f) \begin{cases} = 0 \text{ if } B_{R_i} \text{ is healthy} \\ \neq 0 \text{ if } B_{R_i} \text{ is faulty} \end{cases} \tag{20}$$

4.2 FDL on a star-shaped energy network (SEN)

In a SEN, all the branches of the network are connected to the same node. A fault in one branch can affect all the receivers of the network.
Let us consider the residual values in healthy and faulty situations of the network.

Healthy situation : When the network is not faulty, the successive measurement of the transmission coefficient should be all similar to the reference transmission coefficient. Therefore, the computed residuals are null.

$$\rho_{R_i}(f) = 0 \;\forall\; i \;\in\; \{1;2;\ldots;N+1\} \tag{21}$$

Faulty situation : If a fault occurs, $H_{R_i}^{Test}(f)$ deviates from its reference value, $H_{R_i}^{Ref}(f)$, thus the residuals are not equal to zero. Single and multiple fault scenarios are distinguished.

(1) Single faults scenarios :

- Faulty branch B_S : If a fault occurs in the branch B_S directly linked to the source prior to the node position and all other branches are not faulty, the transmission coefficient between the source and each receiver of the star-shaped network holds the same expression as seen in table 1. Thus, all the expressions of the residuals are identical and independent of the lengths of the branches. The residuals' values are different from zero :

$$\rho_{R_i}(f) = \rho_{R_j}(f) \;\forall\; i,j \in \{1;2;\cdots;N+1\} \tag{22}$$

$$\rho_{R_i}(f) = \left|1 + \frac{Z_f}{2\cdot Z_c} \cdot (1 + \frac{N}{2+N} \cdot e^{-2\cdot\gamma\cdot x_0})\right| - 1 \tag{23}$$
$$\forall\; i \;\in\; \{1;2;\ldots;N+1\}$$

- Faulty branch B_j : If a fault occurs in a branch B_j, directly linked to a receiver R_j, all residuals are different from zero. The residuals associated to healthy branches are equal : $\rho_{R_i}(f) = \rho_{R_m}(f) \;\forall\; i,m \;\in\; \{1;2;\ldots;N+1\} - \{j\}$). The residual expression associated to R_j is different from all others,

$$\rho_{R_j}(f) = \left|1 + \frac{Z_f}{2\cdot Z_c} \cdot (1 + \frac{N}{2+N} \cdot e^{-2\cdot\gamma\cdot x_j})\right| - 1 \tag{24}$$

$$\rho_{R_i}(f) = \left|1 + \frac{(N-3)}{(N+2)} \frac{(Z_f \cdot e^{-2\cdot\gamma\cdot x_j})}{2\cdot Z_c + Z_f\cdot(1+e^{-2\gamma x_j})}\right| - 1 \tag{25}$$
$$\forall\; i \;\in\; \{1;2;\ldots;N+1\} - \{j\}$$

(2) Multiple faults scenarios : Multiple faults may also occur in different branches of the network. It is supposed that the characteristics of the faults (distance to the central node, severity) in the branches are all different. In that case, the residuals associated to the non faulty branches are equal since they are influenced in the same way by the faults on the other branches. All residuals associated to the faulty branches are different. At this stage it is not possible to know if B_S is faulty or not since there is no residual associated

to this branch. In order to know whether the branch B_S is faulty or not, the source may be changed: the source becomes a receiver and one receiver becomes the source.

Remark 1. When all residuals are different between each other, either all branches are faulty, or only one branch is healthy. It is not possible to differentiate these two cases.

Remark 2. In the very particular case where several faults in different branches have the same characteristics (distance to the central node, severity), it is not possible to identify precisely the faulty branches. There will be an ambiguity because several residuals will be equal which may corresponds to faulty or healthy branches. However, this situation may occur very rarely since the effect of the faults must be exactly the same in the different faulty branches.

The algorithm 1 details the proposed detection and localization method for the SEN.

5. APPLICATION CASE STUDY

The validity of this fault detection and localization method is tested in the following using simulated data in the bandwidth $BW = [1 : 0.001 : 100]MHz$. A resistive fault ($5\Omega$) is introduced which has the same effect as a degradation of the conductor of the cable (Kafal and Hassen, 2021).

5.1 Star-shaped energy network

A star-shaped energy network composed of a source, four receivers and five branches is studied. The studied network is presented in Fig. 4 The lengths of the branches B_S, B_1,

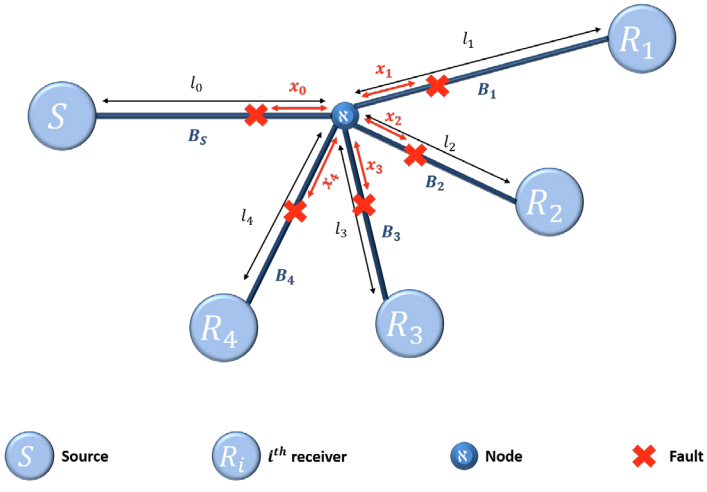

Fig. 4. Star-shaped energy network.

B_2, B_3 and B_4 are respectively $l_0 = 4\ m$, $l_1 = 6\ m$, $l_2 = 2\ m$, $l_3 = 5\ m$ and $l_4 = 3.7\ m$. The distances between the position of the fault and that of the node in each branch are respectively $x_0 = 1.5\ m$, $x_1 = 3.6\ m$, $x_2 = 1.5\ m$, $x_3 = 2.2\ m$ and $x_4 = 1.2\ m$. Each single fault situation of the network is studied separately. The residuals are computed in each situation of the network excluding the healthy situation (it has been verified that all residuals are equal to zero in that situation). Three cases are presented in Fig. 5.

Algorithm 1. Fault detection and localization in a SEN

Detection phase

Input: A set of $N+1$ receivers, $R_i\ \forall i \in \{1; 2; \cdots; N+1\}$
Output: The state of the network

if $\exists \rho_{R_i}(f) \neq 0$ **then**
  Network is faulty;
  Start the localization phase
else
  Network is healthy
end

Localization phase

Input: A set κ, $\kappa \subset \{1; 2; \cdots; N+1\}$, of indices corresponding to equal residuals associated to the healthy branches linked to the receivers, and a set η, such as $\eta := \{1; 2; \cdots; N+1\} - \kappa$.
Output: The set θ of faulty branches.

if $\kappa = \emptyset$ *# All the residuals are different* **then**
  All branches are faulty or only one branch is healthy
else
  if $\eta = \emptyset$ **then**
    $\theta := \{B_S\}$
  else
    Choose two indices, $m, j \in \kappa$ with $m \neq j$
    Exchange R_m with the source # the source becomes the receiver m
    Compute $\rho_{R_m}(f)$ and $\rho_{R_j}(f)$ in the new configuration
    if $\rho_{R_m}(f) = \rho_{R_j}(f)$ **then**
      $\theta := \{B_k\}, \forall k \in \eta$ # Only some receivers' branches are faulty
    else
      $\theta := \{B_S, B_k\}, \forall k \in \eta$ # B_S is faulty as well as some receivers' branches
    end
  end
end

(1) If the fault is inserted in the branch B_S, all the residuals plots are superimposed. Therefore, $\rho_{R_1}(f) = \rho_{R_2}(f) = \rho_{R_3}(f) = \rho_{R_4}(f)$.
(2) If the fault is inserted in the branch B_3, all the residuals plots except the plot of $\rho_{R_3}(f)$ are superimposed. Therefore, $\rho_{R_1}(f) = \rho_{R_2}(f) = \rho_{R_4}(f) \neq \rho_{R_3}(f)$.
(3) The sub-figure (b) represents the variation of the residuals in case of multiple faults. The faults are located at the branch B_1 and B_4. As seen, the plots of $\rho_{R_2}(f)$ and $\rho_{R_3}(f)$ are superimposed ($\rho_{R_2}(f) = \rho_{R_3}(f)$) and $\rho_{R_1}(f) \neq \rho_{R_4}(f) \neq \rho_{R_2}(f)$. The faults can be isolated since the simulation results are consistent with the theoretical part.

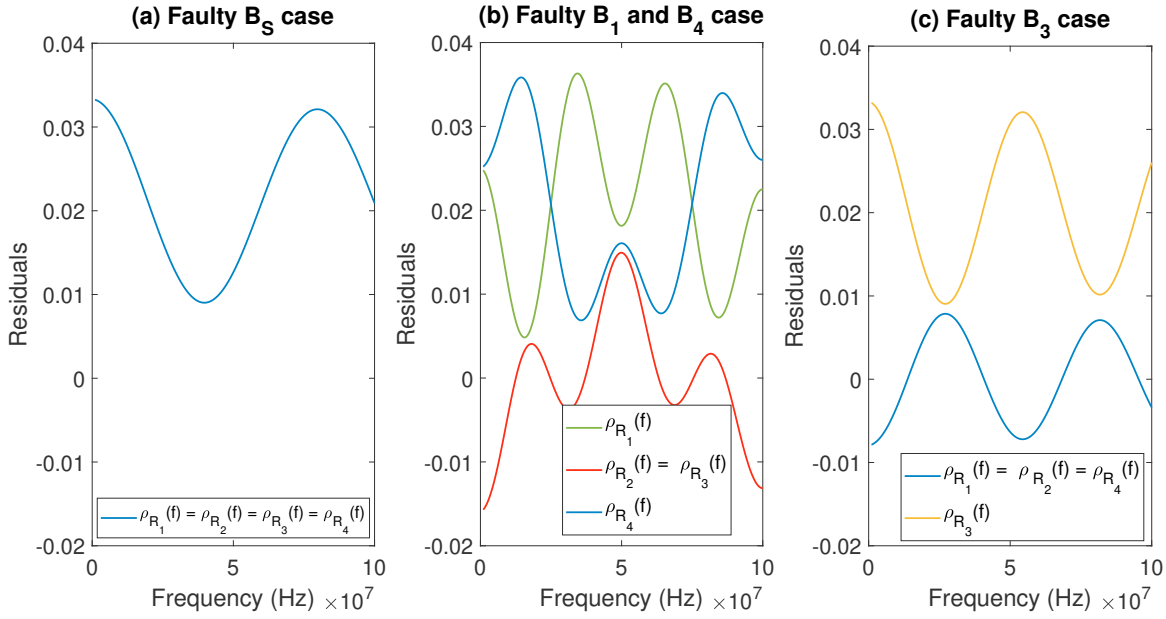

Fig. 5. Variation of the residuals in several possible cases of the SEN.

5.2 Star-shaped communication network

A star-shaped communication network composed of a source, five receivers and five branches is studied. The studied network is presented in Fig. 6 The lengths of the

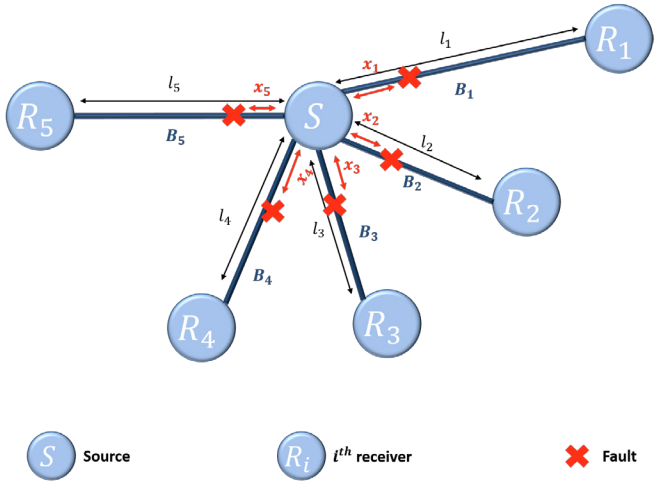

Fig. 6. Star-shaped communication network.

branches B_1, B_2, B_3, B_4 and B_5 are respectively $l_1 = 6\ m$, $l_2 = 2\ m$, $l_3 = 5\ m$, $l_4 = 3.7\ m$ and $l_5 = 4\ m$. The distances between the position of the fault and that of the node in each branch are respectively $x_1 = 3\ m$, $x_2 = 1.5\ m$, $x_3 = 2.7\ m$, $x_4 = 1.2\ m$ and $x_5 = 2.8\ m$. The residuals are computed in two different cases of the network and two cases are presented in Fig. 7.

(1) If the fault is inserted in the branch B_3, all the residuals are null except the one computed at the end of the branch B_3 ($\rho_{R_3}(f) \neq 0$).
(2) If a fault (7 Ω) is inserted in the branch B_5 and another fault (5 Ω) is inserted at the branch B_4, the residuals computed at all the other receivers are null except the one computed at the end of the branches B_5 and B_4 ($\rho_{R_5}(f) \neq \rho_{R_4}(f) \neq 0$).

The localization part is thus straightforward.

6. CONCLUSIONS AND FUTURE WORK

This paper presents a method to detect soft faults and to locate the faulty branches in star-shaped networks. Two types of star-shaped network are considered : *SEN* and *SCN*. A resistor is inserted in series to represent the effect of a soft fault (e.g. series arc or moisture inside a connector) on the transmission coefficient, H_{R_i}, between the source and the receiver R_i. The proposed method is based on a set of residuals deduced from the chain matrix modeling approach. The residuals are computed using RTC and TC which are estimated online through OFDM using PLC. Future work will involve the implementation of the proposed method on a real test bench. The sensitivity of the residual to the faults will be investigated along with the decision procedure in noisy conditions.

REFERENCES

Abdel Karim, A.K., Atoui, M.A., Degardin, V., and Cocquempot, V. (2021a). Fault detection and localization in vehicular embedded network using power line communication. In *The International Conference on Systems and Control (ICSC'2021), Caen, France, November 2021.*

Abdel Karim, A.K., Atoui, M.A., Degardin, V., and Cocquempot, V. (2021b). Fault detection and localization in y-shaped network through power line communication. In *The conference on Control and Fault-Tolerant Systems (SysTol'21), Saint-Raphael, France, September 2021.*

Abdel Karim, A.K., Degardin, V., Cocquempot, V., and Atoui, M.A. (2021c). Soft fault detection and localization in an unshielded twisted pair network using power line communication. In *7th International Conference on Vehicle Technology and Intelligent Transport Systems (VEHITS), page 104380, Online, Portugal, April 2021.*

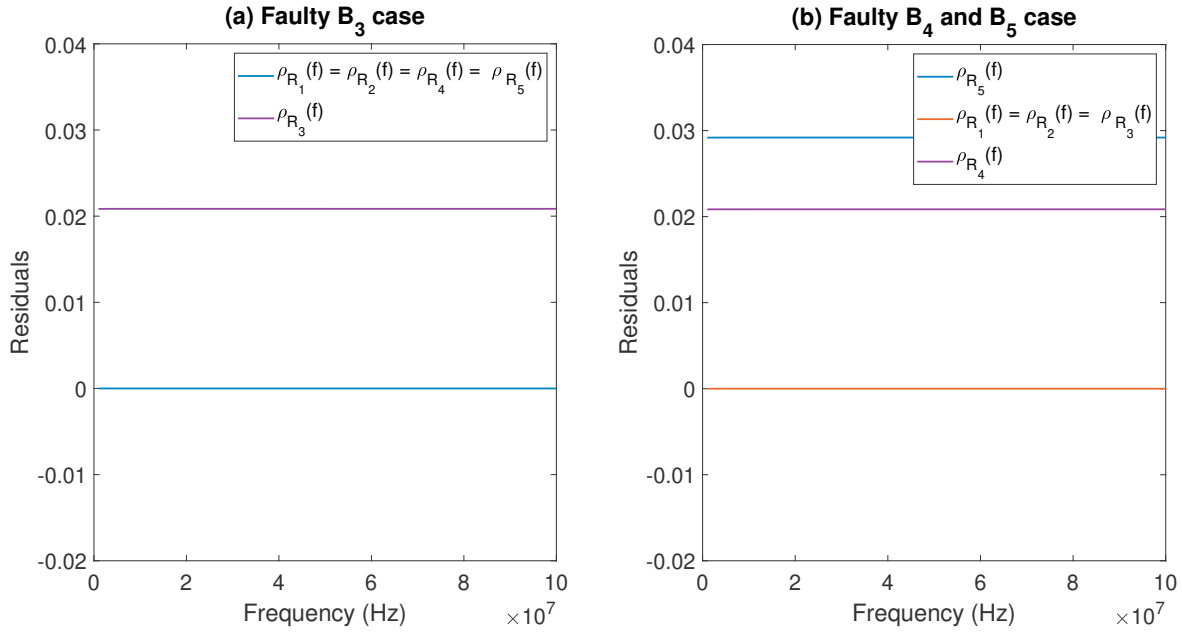

Fig. 7. Variation of the residuals in several possible cases of the SCN.

Auzanneau, F. (2013). Wire troubleshooting and diagnosis: Review and perspectives. *Progress In Electromagnetics Research B*, 49, 253–279.

Bahl, I. (2009). *Fundamentals of RF and microwave transistor amplifiers*. John Wiley & Sons.

Dubickas, V. (2006). *On-line time domain reflectometry diagnostics of medium voltage XLPE power cables*. Ph.D. thesis, Kungliga Tekniska Hogskolan Electrical Engineering.

Espina, J., Falck, T., Panousopoulou, A., Schmitt, L., Mülhens, O., and Yang, G.Z. (2014). Network topologies, communication protocols, and standards. In *Body sensor networks*, 189–236. Springer.

Furse, C.M., Kafal, M., Razzaghi, R., and Shin, Y.J. (2020). Fault diagnosis for electrical systems and power networks: A review. *IEEE Sensors Journal*, 21(2), 888–906.

Hsieh, M.H. and Wei, C.H. (1998). Channel estimation for ofdm systems based on comb-type pilot arrangement in frequency selective fading channels. *IEEE Transactions on Consumer Electronics*, 44(1), 217–225.

Huo, Y., Prasad, G., Atanackovic, L., Lampe, L., and Leung, V.C. (2019). Cable diagnostics with power line modems for smart grid monitoring. *IEEE Access*, 7, 60206–60220.

Huo, Y., Prasad, G., Lampe, L., and Leung, V.C. (2020). Advanced smart grid monitoring: Intelligent cable diagnostics using neural networks. In *2020 IEEE International Symposium on Power Line Communications and its Applications (ISPLC)*, 1–6. IEEE, Málaga, Spain, May 2020.

Kafal, M. and Hassen, W.B. (2021). Method for characterising a fault in a transmission line network with unknown topology. US Patent App. 17/253,099.

Lallbeeharry, N., Mazari, R., Dégardin, V., and Trebosc, C. (2018). Plc applied to fault detection on in-vehicle power line. In *2018 IEEE International Symposium on Power Line Communications and its Applications (ISPLC)*, 1–5. IEEE, Manchester, United Kingdom, April 2018.

Lehmann, A.M., Raab, K., Gruber, F., Fischer, E., Müller, R., and Huber, J.B. (2016). A diagnostic method for power line networks by channel estimation of plc devices. In *2016 IEEE International Conference on Smart Grid Communications (SmartGridComm)*, 320–325. IEEE, Sydney, NSW, Australia, Nov. 2016.

Mlỳnek, P., Misurec, J., Koutnỳ, M., and Orgon, M. (2011). Power line cable transfer function for modelling of power line communication system. *Journal of Electrical Engineering*, 62(2), 104.

Paul, C.R. (2007). *Analysis of multiconductor transmission lines*. John Wiley & Sons.

Sommervogel, L. (2020). Various models for faults in transmission lines and their detection using time domain reflectometry. *Progress In Electromagnetics Research C*, 103, 123–135.

Yang, F., Ding, W., and Song, J. (2013). Non-intrusive power line quality monitoring based on power line communications. In *2013 IEEE 17th International Symposium on Power Line Communications and Its Applications*, 191–196. IEEE, Johannesburg, South Africa, March 2013.